Bull. Chem. Soc. Ethiop. **2024**, 38(6), 1725-1742.
DOI: https://dx.doi.org/10.4314/bcse.v38i6.18

ISSN 1011-3924
Printed in Ethiopia
Online ISSN 1726-801X

SYNTHESIS, SPECTROSCOPIC CHARACTERIZATION AND ANTIMICROBIAL EVALUATION OF METAL COMPLEXES WITH N-(2-AMINOPHENYL)-4-(PENTYLOXY) BENZAMIDE COMPOUND LIGAND

Shaimaa M. Faheem[1], Awatef A. Masoud[2], Abdou S. El-Tabl[3*], Marwa H. Gendia[3] and Sara M. Younes[4]

[1]High Technology Institute of Applied Health Sciences, Badr Academy, Badr City, Egypt
[2]Department of Chemistry, Faculty of Science, Tobruk University, Libya
[3]Department of Chemistry, Faculty of Science, El-Menoufia University, Shebin El-Kom, Egypt
[4]Chemical Engineering Department, Borg El Arab Higher Institute Engineering and Technology, Alexandria, Egypt

(Received May 15, 2024; Revised July 30, 2024; Accepted August 1, 2024)

ABSTRACT. New metal complexes of Mn(II), Cu(II), Ni(II), Cd(II) and Zn(II) of (N-(2-aminophenyl)-4-(pentyloxy) benzamide were prepared and characterized, discovering new compounds with therapeutic value against microbial ligand and it's complexes were characterized using various analytical techniques. The electron spin resonance spectra of complex (**4**), $[(L)(Cu)(OAc)_2(H_2O)_2].2H_2O$, complex (**5**), $[(L)(Cu)(Br)_2(H_2O)_2].2H_2O$ showed axial octahedral structure however complex (**10**) $[(L)(Cu)(SO_4)(H_2O)_3].3H_2O$ showed compressed tetragonal geometry and complex (**9**) $[(L)(Mn)(Cl)_2(H_2O)_2].H_2O$ showed isotropic type the electronic spectra of copper(II) complexes (**4**), (**5**), (**7**) and (**10**) nearly showing bands at (240-270) nm, (300-380) nm, (420-573) nm and (610-770) nm ranges. For metal complexes, Mn(II) complex (**2**) is most sensitive complex against *Bacillus subtilis*, *Staphylococcus aureus*, *Escherichia coli*, and *Pseudomonas Aeruginosa*, with 21, 25, 21, 22 mm, respectively inhibition zone whereas, Zn(II) complex (**10**) recorded the highest antimicrobial activity against *Streptococcus aureus*, The orders of the antimicrobial activity were *Bacillus subtilis:* Standard drug > Mn(II) complex (**2**) > Zn (II) complex (**11**) > Cd(II) complex (**6**) > Cu(II) complex (**5**, **7**) > Cu(II) complex (**4**) > Cu(II) complex (**10**) > The ligand [L] (**1**) where the standard drugs were kanamycin (positive controls) and ampicillin (negative control).

KEY WORDS: Metals complexes, Spectra, Magnetism, Antibacterial activity, Ampicillin

INTRODUCTION

Bioinorganic chemistry is a rapidly growing area which explores the use of inorganic and organo-metallic compounds in biological application. Major causes of morbidity and mortality throughout the globe caused by microbial pathogens. Different metal complexes have influential biological roles and therefore their design may help in developing new drugs. Organic compounds containing nitrogen and their metal complexes have a wide range of biological activities such as antibacterial, antifungal, antitumor and antiviral [1]. Metals are reported to target multiples cellular sites such as cellular membrane, genetic materials, and reactive oxygen spies – mediated cellular pleiotpic that effect on specific targets on biochemical pathways such as replication, transcription translocation and enzymatic reaction [2]. Benozimide are important and used owing to their high thermo-oxidative stability, chemical resistance properties with the continued growth of the medical and drugs industry. In organic chemistry, a Schiff base (named after Hugo Schiff) is a compound with the general structure $R^1R^2C{=}NR^3$ (R^3 = alkyl or aryl, but not hydrogen) [3]. They can be considered a sub-class of imines, being either secondary ketimines or secondary aldimines depending on their structure. Anil refers to a common subset of Schiff bases: imines derived from anilines [4]. The term can be synonymous with azomethine which refers specifically to secondary aldimines (i.e. R−CH=NR' where R' ≠ H). Microbial infections have been frightening human life over a centuries. Microorganism such as *Enterococcus*,

*Corresponding authors. E-mail: ch_sara2011@yahoo.com

Staphylococcus, *Enterobacter*, *Klebsiella pneumoniae*, *Acinetobacter* and *Pseudomonas aeruginosa* are the microorganism of utmost concern [5]. Moreover, antimicrobial drugs have caused a dramatic change not only of the treatment of infectious diseases but of a fate of mankind. Antimicrobial chemotherapy made notable advances, resulting in the excessively optimistic view that infectious diseases would be conquered in the near future. Nevertheless, in truth, budding and re-emerging infectious diseases have left us facing a counter charge from infections. Infections with drug resistant organisms remain an important dilemma in clinical perform that is difficult to resolve. If an improper antimicrobial agent is selected for the cure of infection with drug-resistant microorganisms, the therapy may not attain valuable effect, and moreover, may direct to a worse diagnosis [6]. Hence, there is an urgent need to development to new, wide spectrum antimicrobial agents that could target and eliminate antidrug resistance microbes. A renewed interest in metal complexes as antimicrobial and biocidal agents reflected in hopes that less resistance will evolve. In this study, a flexible new benzamide compound and its complexes were synthesized and characterized and also antibacterial effect was studied in comparison with ampicillin and kanamycin (against gram-positive and gram-negative) bacterial strains of clinical importance using disc diffusion test.

EXPERIMENTAL

Instrumentation and measurements

The ligand and its metal complexes were analyzed for determining the components: C, H, N and Cl at the Microanalytical Center, Cairo University, Egypt. Standard analytical methods were used to determine the metal ion content. ^{1}H-NMR spectra were obtained on Bruker 400 MHz spectrometers [7]. Chemical shifts (ppm) are reported relative to TMS, IR spectra of the ligand and its metal complexes were measured using KBr discs by a Jasco FT/IR 300E Fourier transform infrared spectrophotometer covering the range 400-4000 cm^{-1} [8]. Electronic spectra in the 200-900 nm regions were recorded on a Perkin-Elmer 550 spectrophotometer. The thermal analyses ((differential thermal analysis) DTA and (thermogravimetric analysis) TGA) were carried out on a Shimadzu DT-30 thermal analyzer from room temperature to 800 ºC at a heating rate of 10 ºC /min. Magnetic susceptibilities were measured at 25 ºC by the Gouy method [9] using mercuric tetrathiocyanatocobaltate(II) as the magnetic susceptibility standard. Diamagnetic corrections were estimated from Pascal's constant [10]. The molar conductance of 10^{-3} M of the complexes in DMSO (dimethyl sulfoxide) solution was measured at 25 ºC with Bibby conductor type (Mid Circuit Interrupter MCI) mass spectra of the ligand and some of its metal complexes were measured using JEUL MS-AX500 mass spectrometer provided with data system. ESR spectra were recorded using a Varian E-109 spectra photometer. (2,2-Diphenyl-1-picrylhydrazyl) DPPH was used as a standard material.

Synthesis of ligand

The ligand, (HL) was prepared by dropwise addition ethanolic solution of sodium salt of methyl benzoate (30.0 g, 0.17 mol) in ethanolic solution of iodopentane (34.30 g, 0.17 mol) then the product added to the mixture was refluxed with stirring for one hour and then *o*-phenylene diamine (10.0 g and 0.09 mol) dissolved in 20 cm^{3} of ethanol solution was added. The mixture was refluxed with stirring for 2 hours and then left to cool at room temperature and filtered off the formed precipitate and leave it to dry at room temperature. The solid product was filtered off, and then dried under vacuum over anhydrous $CaCl_2$ to give the ligand [10].

Synthesis of metal complexes

*Preparation of metal complexes (**2-11**)*

Complexes were prepared by refluxing with stirring a hot ethanolic 30 mL solution of the ligand (1.0 g, 0.003 mol) with a hot ethanolic solution 30 mL of the metal salts, (0.58 g, 0.003 mol) of $Mn(OAc)_2].3H_2O$ (1L:1M), complex (**2**), (0.59 g, 0.003 mol) $Ni(OAc)_2.4\ H_2O$ (1L:1M), complex (**3**), (0.62 g, 0.003 mol) of $Cu(OAc)_2].H_2O$ (1L:1M), complex (**4**), (0.74 g, 0.003 mol) of $CuBr_2$ (1L:1M), complex (**5**), (0.61, 0.003 mol) of $CdCl_2.\ H_2O$ (1L:1M), complex (**6**), (0.45 g, 0.003 mol) of $CuCl_2.\ H_2O$ (1L:1M), complex (**7**) , (0.43 g, 0.003 mol) of $NiCl_2].6H_2O$ (1L:1M), complex (**8**), (0.42 g, 0.003 mol) $MnCl_2.4H_2O$, (1L:1M), complex (**9**) , (0.53 g, 0.003 mol) of $CuSO_4.5H_2O$ (1L:1M), complex (1**0**) , (0.54 g, 0.003 mol) of $ZnSO_4.H_2O$ (1L:1M), complex (**11**). The reaction mixtures were refluxed with stirring for 1–3 h range, depending on the nature of the metal ion and the anion. The precipitates so formed were filtrated off, washed with ethanol and dried in desiccators using anhydrous CaCl antimicrobial activity of the tested samples was determined using a modified Kirby-Bauer disc diffusion method [11]. The antibacterial activity of synthesized compounds was studied by the disc diffusion method against the following pathogenic organisms. The gram-positive bacteria screened were *Staphylococcus aureus* NCCS 2079 and *Bacillus cereus* NCCS 2106. The gram-negative bacteria screened were *Escherichia coli* and *Pseudomonas aeruginosa*. The synthesized compounds were used at the concentration of 250 µg/mL and 500 µg/mL using DMSO as a solvent. The Cefaclor 10 µg/disc was used as a standard. (Microanalysis Center, College of African Studies, Cairo University, Egypt).

RESULTS AND DISCUSSION

Metal complexes were colored, crystalline solids, non-hygroscopic and had high stability in air at room temperature without decomposition for a long time. The complexes were insoluble in water, ethanol, methanol, benzene, toluene, acetonitrile and chloroform, but appreciably soluble in both (DMF) and (DMSO). The analytical and physical data (Table 1) and spectral data, (Tables 2-4) agree well with the proposed structures (Figure 1 and 2). The elemental analyses indicated that, all complexes were found to (1L: 1M) molar ratios. Synthesis of the ligand is shown in Figure 1.

Conductance measurements

The molar conductivities of the complexes were measured in DMSO solvent with 1.0×10^{-3} M. Electrolytes are usually much worse conductors of electricity than metals. Their conductivity is less than 100 [S/m], whereas the metallic conductors show conductivity of the order of 106 - 108 [S/m]. With the increasing temperature the electric resistivity of electrolytes generally decreases. The low magnitudes of molar conductivities $\Omega^{-1}cm^2mol^{-1}$ (listed in Table 1) indicated that, all of the complexes possess non-electrolytic nature [12]. These values agree well with the analytical data assigned to the involvement of the anions groups in the metal coordination.

Mass spectra

Mass spectrometry was used to confirm the molecular ion peaks of ligand HL, Schiff-base and also to investigate the fragment species [13]. The recorded mass spectrum of HL ligand revealed molecular ion peak confirms strongly the proposed formula. It showed a molecular ion peak at m/z 298 amu, confirming its formula weight (FW 298) and the purity of the ligand prepared. The prominent mass fragmentation peaks observed at m/z = 51, 65, , 77, 91, 102, 120, 152, 166, 181 196, 210, and 298, amu corresponding to C_4H_3, C_5H_5, C_6H_5, C_6H_5N, $C_6H_{16}N$, $C_6H_{18}NO$,

$C_6H_{20}N_2O_2$, $C_7H_{22}N_2O_2$, $C_{12}H_9N_2$, $C_{12}H_8N_2O$, $C_{13}H_{10}N_2O$, and $C_{18}H_{22}N_2O_2$ moieties, respectively, supported the suggested structure of the ligand (Table 2, i).

The mass spectrum of the $[(HL)(Ni)(OAc)_2(H_2O)_2].2H_2O$ complex (**3**) showed the molecular ion peak at *m/z* 547 amu, confirming its formula weight (F.W. 547).The mass fragmentation patterns observed at *m/z* = 55, 77, 121 , 152, 167, 210, 262, 285, 372, 437, 458, and 547 amu correspond to C_4H_7, C_6H_5, C_8H_9O, $C_8H_{10}NO_2$, $C_8H_{11}N_2O_2$, $C_9H_{10}N_2O_4$, $C_{11}H_6N_2O_6$, $C_{11}H_{13}N_2O_7$, $C_{15}H_{20}N_2O_9$, $C_{20}H_{25}N_2O_9$, $C_{20}H_{30}N_2O_{10}$, and $C_{22}H_{36}N_2NiO_{10}$ moieties, respectively, strongly supported the suggested structure of the complex. (Table 2, i).

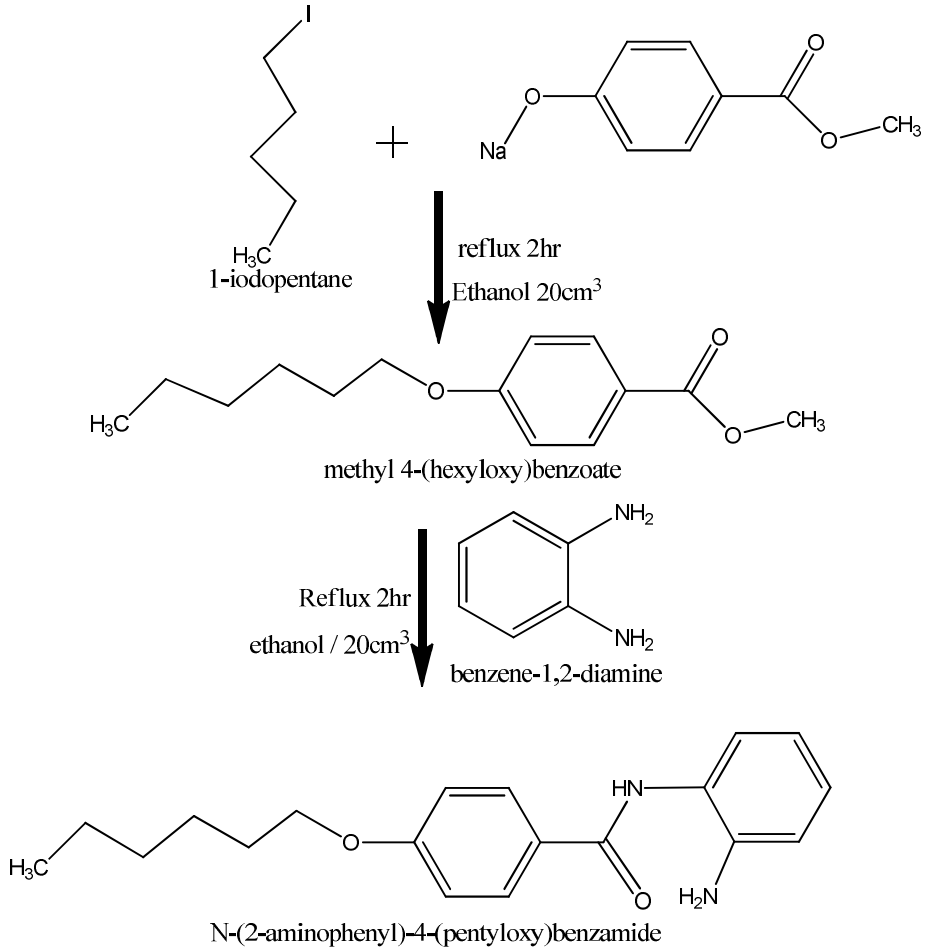

Figure 1. Synthesis of ligand [HL] (**1**).

Table 1. Analytical and Physical Data of the Ligand [HL] (1) and its Metal complexes.

No.	Ligand/complexes	Color	FW	m.p. (ºC)	Yield (%)	Anal. /found (calc.) (%)					Molar conductance*
						C	H	N	M	Cl/Br	
(**1**)	[L] $C_{18}H_{22}N_2O_2$	Reddish brown	298.38	>300	75	72.0 (72.46)	7.55(7.43)	9.12(9.39)	-	-	
(**2**)	$[(HL)(Mn)(OAc)_2(H_2O)_2].H_2O$ $C_{22}H_{34}MnN_2O_9$	Purple gray	525.45	>300	70	50.11 (50.29)	6.32(6.52)	5.12(5.33)	10.21(10.46)	-	5.06
(**3**)	$[(HL)(Ni)(OAc)_2(H_2O)_2].2H_2O$ $C_{22}H_{36}N_2NiO_{10}$	Blue	547.22	>300	75	47.98 (48.29)	6.42(6.63)	4.82(5.12)	10.52 (10.73)	-	6.3
(**4**)	$[(HL)(Cu)(OAc)_2(H_2O)_2].2H_2O$ $C_{22}H_{36}CuN_2O_{10}$	Greenish Yellow	552.07	>300	78	47.65(47.86)	6.32(6.57)	4.81(5.07)	11.23 (11.51)	-	4.97
(5)	$[(HL)(Cu)(Br)_2(H_2O)_2].2H_2O$ $C_{18}H_{30}Br_2CuN_2O_6$	Gray	593.79	>300	80	36.31 (36.41)	4.71(5.09)	4.53(4.72)	10.51 (10.70)	26.72(26.91)	8.70
(**6**)	$[(HL)(Cd)(Cl)_2(H_2O)_2].2H_2O$ $C_{18}H_{30}CdCl_2N_2O_6$	Brown	553.76	>300	73	38.78 (39.04)	5.15(5.46)	4.78(5.06)	19.92(20.30)	12.65(12.80)	5.37
(**7**)	$[(HL)(Cu)(Cl)_2(H_2O)_2].2H_2O$ $C_{18}H_{30}Cl_2CuN_2O_6$	Dark green	504.89	>300	85	42.61 (42.82)	5.71(5.99)	5.21(5.55)	12.42 (12.59)	13.92(14.04)	345
(**8**)	$[(HL)(Ni)(Cl)_2(H_2O)_2].H_2O$ $C_{18}H_{28}Cl_2N_2NiO_5$	Gray	482.02	>300	75	44.68 (44.85)	5.71(5.85)	5.51(5.81)	11.87 (12.18)	14.58(14.71)	4.75
(**9**)	$[(HL)(Mn)(Cl)_2(H_2O)_2].H_2O$ $C_{18}H_{28}Cl_2MnN_2O_5$	Dark brown	478.27	>300	65	44.89 (45.20)	5.35(5.90)	5.69(5.86)	11.1(11.49)	14.67(14.83)	5.88
(**10**)	$[(HL)(Cu)(SO_4)(H_2O)_3].3H_2O$ $C_{18}H_{34}CuN_2O_{12}S$	Dark brown	566.08	>300	65	37.87(38.19)	5.92(6.05)	4.56(4.95)	10.92 (11.23)	-	5.88
(**11**)	$[(HL)(Zn)(SO_4)(H_2O)_3].3H_2O$ $C_{18}H_{34}N_2O_{12}SZn$	Dark brown	567.92	>300	65	37.92 (38.07)	5.82(6.03)	4.78(4.93)	11.21 (11.51)	-	5.88

*$\Lambda m(\Omega^{-1}cm^2mo^{-1})$.

Table 2, i. The mass spectrum of ligand [HL] (**1**) and Ni(II) complex (**3**).

Ligand [HL] (**1**)			Ni(II) complex (**3**)		
m/z	Rel. Int.	Fragment	m/z	Rel. Int.	Fragment
51	50	C_4H_3	55	3.06	C_4H_7
65	51	C_5H_5	77	0.38	C_6H_5
77	100	C_6H_5	121	0.40	C_8H_9O
91	40	C_6H_5N	152	0.09	$C_8H_{10}NO_2$
102	32	$C_6H_{16}N$	167	0.11	$C_8H_{11}N_2O_2$
120	35	$C_6H_{18}NO$	210	0.17	$C_9H_{10}N_2O_4$
152	20	$C_6H_{20}N_2O_2$	262	0.23	$C_{11}H_6N_2O_6$
166	25	$C_7H_{22}N_2O_2$	285	0.10	$C_{11}H_{13}N_2O_7$
181	40	$C_{12}H_9N_2$	372	0.11	$C_{15}H_{20}N_2O_9$
196	50	$C_{12}H_8N_2O$	437	0.13	$C_{20}H_{25}N_2O_9$
210	61	$C_{13}H_{10}N_2O$	458	0.42	$C_{20}H_{30}N_2O_{10}$
298	23	$C_{18}H_{22}N_2O_2$	547	0.45	$C_{22}H_{36}N_2NiO_{10}$

The mass spectrum of the $[(HL)(Cu)(OAc)_2(H_2O)_2].2H_2O$ complex (**4**) showed the molecular ion peak at *m/*z 552 amu, confirming its formula weight (F.W. 552).The mass fragmentation

patterns observed at *m/z* = 55 71, 93 , 121, 152, 251, 301, 368, 412, 501 and 552 amu correspond to C_4H_7, C_5H_{11}, C_7H_9, $C_8H_{11}N$, $C_9H_{14}NO$, $C_{15}H_{11}N_2O_2$, $C_{16}H_{17}N_2O_4$, $C_{18}H_{28}N_2O_6$, $C_{19}H_{28}N_2O_8$, $C_{18}H_{34}CuN_2O_{10}$ and $C_{22}H_{36}CuN_2O_{10}$ moieties, respectively, strongly supported the suggested structure of the complex, (Table 2 ii). However, the mass spectrum of the $[(L)(Cu)(Cl)_2(H_2O)_2].2H_2O$ complex (**7**) showed the molecular ion peak at *m/z* 504 amu, confirming its formula weight (F.W. 504). The mass fragmentation patterns observed at *m/z* = 55, 71, 121, 152, 181, 210, 274, 318, 351, 504 amu correspond to C_4H_7, C_6H_5, C_8H_9O, $C_8H_{10}NO_2$, $C_8H_{11}N_2O_2$, $C_9H_{10}N_2O_4$, $C_{12}H_6N_2O_6$, $C_{15}H_{14}N_2O_6$, $C_{17}H_{23}N_2O_6$, $C_{18}H_{28}ClCuN_2O_6$ and $C_{18}H_{30}Cl_2CuN_2O_6$ moieties, respectively, supported the suggested structure of the complex (Table 2, ii). Due to the difference in molar conductivities, function group, and mass spectra so metal complexes have specific steric and electronic effects that lead to different mechanisms of action.

Table 2, ii. The mass spectrum of Cu(II) complex (**4**) and Cu(II) complex (**7**).

Cu (II) complex (4)			Cu(II) complex (7)		
M/Z	Rel. Int.	Fragment	m/z	Rel. Int.	Fragment
55	51	C_4H_7	55	3.06	C_4H_7
71	65	C_5H_{11}	71	0.38	C_6H_5
93	77	C_7H_9	121	0.40	C_8H_9O
121	102	$C_8H_{11}N$	152	0.09	$C_8H_{10}NO_2$
152	120	$C_9H_{14}NO$	181	0.11	$C_8H_{11}N_2O_2$
251	152	$C_{15}H_{11}N_2O_2$	210	0.17	$C_9H_{10}N_2O_4$
301	166	$C_{16}H_{17}N_2O_4$	274	0.23	$C_{12}H_6N_2O_6$
368	181	$C_{18}H_{28}N_2O_6$	318	0.10	$C_{15}H_{14}N_2O_6$
412	196	$C_{19}H_{28}N_2O_8$	351	0.11	$C_{17}H_{23}N_2O_6$
501	210	$C_{18}H_{34}CuN_2O_{10}$	466	0.42	$C_{18}H_{28}Cl\,CuN_2O_6$
552	298	$C_{22}H_{36}CuN_2O_{10}$	504	0.45	$C_{18}H_{30}Cl_2CuN_2O_6$

Proton nuclear magnetic resonance spectra (^{1}H-NMR)

The ^{1}H-NMR spectra of ligand (**1**) and its complexes Cd(II) (**6**) and Zn(II) complex (**10**) in deuterated DMSO showed peaks consistent with the proposed structures. The ^{1}H-NMR spectrum of the ligand showed chemical shift observed as singlet at 3.7 ppm was attributed to the methyl protons. However, the chemical shifts appeared as a singlet at 5.32 and 8.9 ppm were attributed to the proton of NH_2 and NH group. A set of signals appeared as multiples in the 6.8-7.4 ppm range, corresponding to protons of aromatic rings. By comparison the ^{1}H- NMR of the ligand and the spectra of the Cd(II) (**6**), Zn(II) (**11**) complexes it was observed the presence of the signal shifted to downfield shift characteristic to the (OH) group indicating that, the ligand bonded with the ions. In addition, there was not a significant downfield shift of the azomethine proton signal and one from (NH) groups relative to the free ligand clarified that, the metal ions were not coordinated to the azomethine nitrogen atom and NH nitrogen atom. The complexes showed news signal at 1.611 ppm may be due to protons of acetate group [14].

IR spectra

FT-IR spectrum of Schiff base ligand, peaks were appeared at 3200 cm $^{-1}$ and 1612 cm $^{-1}$ due to (NH_2) and (C=O) respectively [15]. These frequencies were shifted in the lower frequency at (3120-3195 cm $^{-1}$) and (1604-1612 cm $^{-1}$) ranges in metal complexes confirmed the (NH_2) and (C=O) groups were coordinated to central metal ions [16]. A broad peak appeared at 1319 cm $^{-1}$ in free ligand was due to ether oxygen atom. However, in metal complexes, it was appeared at 1706-1689 cm^{-1} range, and the new frequencies are observed at (560-519 cm $^{-1}$) and (586-619 cm^{-1}) ranges were assigned to ν(M-N) and ν(M-O) vibrations frequencies which designates (NH_2) and (C=O) were involved in the coordination of central metal ion. A new peak observed at (1435-

1461 cm $^{-1}$) ranges (symmetry) and (1377-1325 cm $^{-1}$) ranges (asymmetry) due to presence of CH_3COO^- ion in the acetate complexes (**2-4**). The sulfate complexes (**10**) and (**11**) showed bands at (1110, 1038, 1070, 690 cm^{-1}) and (1105, 1040, 1055, 700 cm^{-1}), respectively, which assigned to monodentate sulphate group. The chloride complexes (**6-9**) showed bands at (450-466 cm^{-1}), which assigned to chloride group. H-bonding peaks complexes at 3630-3310 cm^{-1} range, however, the complexes showed hydration and coordination water at 3560-3310 cm^{-1} range [17]. The IR data were represented in Table 3.

Table 3. IR frequencies of the bands (cm^{-1}) of Ligand [HL], (**1**) and its Metal complexes.

No.	ν(H_2O)	ν(H-b)	ν(NH_2)	ν(NH)	ν(CH_2) $_4CH_3$	ν (C=O) amide	ν – O-	ν(Ar)	ν(C-N)	ν(SO_4), ν($OAc)_2$	ν(M-Br), ν(M-Cl)	ν(M-O)	ν(M-N)
L(**1**)		3620 - 3350 3540 - 2465	3465 3420 1590	3200	3053 2930 2860	1612	1700	1481 752	1036	--	--	--	--
$Mn(OAc)_2$ (**2**)	3510 - 3365 3300 - 3150	3625 - 3310 3300 - 2920	3400 3425 1573	3195	3056 2924 3000	1605	1706	1487, 751	1030	1461 1377	--	609	540 [1]
$Ni(OAc)_2$ (**3**)	3500 - 3330 3320 - 3125	3620 - 3310 3300 - 2760	3440 3400 1520	3150	3035 2928 2860	1605	1702	1437, 750	1035	1435 1334	--	619	542
$Cu(OAc)_2$ (**4**)	3530 - 3320 3310 - 3160	3600 - 3225 3220 - 2820	3434 3395 1521	3142	3052 2925 2880	1607	1689	1470, 750	1030	1455 1325	--	606	535
$CuBr_2$ (**5**)	3560 - 3380 3345 - 3130	3600 - 3350 3340 - 2950	3420 3385 1530	3195	3050 2923 2870	1607	1701	1462, 751	1035	--	411	600	537
$CdCl_2$ (**6**)	3520 - 3310 3300 - 3100	3630 - 3260 3250 - 2570	3415 3325 1486	3120	3050 2930 2860	1604	1693	1456, 746	1036	--	466	586	519
$CuCl_2$ (**7**)	3510 - 3350 3340 - 3100	3600 - 3320 3310 - 2780	3410 3398 1530	3135	3050 2928 2865	1608	1699	1447, 750	1041	--	450	617	540
$NiCl_2$ (**8**)	3510 - 3330 3320 - 3125	3610 - 3320 3310 - 2650	3408 3380 1516	3135	3049 3012 2925	1605	1693	1443, 750	1033	--	455	610	540
$MnCl_2$ (**9**)	3510 - 3335 3300 3150	3615 - 3220 3210 - 2670	3414 3385 1531	3188	3056 2955 3860	1604	1696	1477 750	1038	--	463	614	542
$CuSO_4$ (**10**)	3530 - 3310 3300 - 3110	3610 - 3335 3330 - 2750	3406 3385 1530	3165	3062 2950 3875	1612	1705	1479, 754	996	1110, 1038, 1070, 690	--	603	535
$ZnSO_4$ (**11**)	3530 - 3330 3320 - 3150	3620 - 3320 3310 - 2750	3420 3392 1530	3130	3060 2950 3850	1609	1698	1465 748	1040	1105, 1040, 1055, 700	--	615	560

Electronic spectra and magnetic moments

The electronic absorption spectral data of the ligand (**1**) and its metal complexes in DMF were listed in Table 4. The ligand showed two bands at 290 and 310 nm. The first band may be assigned to $\pi\rightarrow\pi^*$, $n\rightarrow\pi^*$ and charge transfer transitions of the amines and carbonyl groups [18]. These bands were shifted to lower energy upon complex formation, indicating participation of these groups in coordination with the metal ions. The electronic spectra of copper(II) complexes (**4**), (**5**), (**7**) and (**10**) were nearly identical and showing bands at 270, 265, 350, 570, 660, 770) nm, (270, 302, 435, 562, 600) nm, (268, 301, 321, 435, 571, 603) nm and (263, 275, 305, 360, 440, 560, 610) nm. The first two bands were assigned to intraligand transitions; however, the other bands ranges are assigned to $^2B_{1g}\rightarrow{}^2A_{1g}$ $\nu_1(dx^2\text{-}y^2\rightarrow dz^{2\text{-}})$, $^2B\rightarrow{}^2B_{2g}$, $\nu_2(dx^2\text{-}y^2\rightarrow dxy)$, and $^2B_{1g}\rightarrow{}^2Eg$, $\nu_3(dx^2\text{-}y^2\rightarrow dxy, dyz)$ transitions, respectively. These transitions indicated that, the copper(II) ion had a tetragonally distorted octahedral geometry. This could be due to the Jahn-Teller effect that operated on the d^9 electronic ground state of six coordinate system, elongating one trans pair of coordinate bonds and shortening the remaining four ones [19]. The magnetic moments for copper(II) complexes at room temperature were in the 1.69-1.71 BM range, supporting that the complexes had octahedral geometry [20]. Nickel(II) complexes (**3**) and (**8**) displayed bands (265, 306, 462, 548, 600 and 745 nm) and (270, 290, 380, 450, 601, and 750) nm, respectively. The first bands were corresponding to intra ligand transitions, however the other bands due to $^3A_{2g}(F)\rightarrow{}^3T_{2g}$ (ν_1), $^3A_{2g}(F)\rightarrow{}^3T_{2g}(F)$ (ν_2), and $^3A_{2g}(F)\rightarrow{}^3T_{1g}(P)$ ν_3 transitions, distorted indicating octahedral nickel(II) complexes, the ν_2/ν_1 was 1.36 and 1.60 indicating distorted octahedral structures [21]. The values of magnetic moments for nickel(II) complexes (**3**) and (**8**) were in the 3.12 and 3.21 however, manganese(II) complexes (**2**) and (**9**) showed bands 265, 305, 470, 579, 605 and 263, 300, 370, 450, 573, 610 nm and the first band are within the ligand however, the other bands were due to $6A_1g\rightarrow4Eg$, $6A_1g\rightarrow4T_2g$ and $6A_1g\rightarrow4T_1g$ transitions indicating octahedral geometry for the complexes (**2**) and (**9**) were 6.32 and 6.23 B.M. confirming high spin Mn(II) octahedral structure [22]. Which were consistent with two unpaired electrons state, confirming octahedral geometry around nickel(II) ion [23]. The observed bands for zinc(II) complexes (**11**), (Table 4) are due to intra ligand transitions within the ligand and show diamagnetic property [24].

Table 4. The electronic spectra (nm) and magnetic moments (B.M.) for the ligand [L](**1**), and its complexes.

No.	λ_{max} (nm)	μ_{eff} in B.M.	ν_2/ν_1
(**1**)	290 nm (log ε = 3.98), 310 nm (log ε = 4.25)	-	
(**2**)	265, 305, 470, 579, 605	6.32	
(**3**)	265, 306, 462, 548, 600,745	1.36	
(**4**)	270, 265, 350, 570, 660, 770	3.12	
(**5**)	270, 302, 435, 562, 600	1.71	
(**6**)	265, 307, 335	Diamag.	
(**7**)	268, 301, 321, 435, 571, 603	1.69	
(**8**)	270, 301, 380, 450, 600,750	3.21	
(**9**)	263, 300, 370, 450, 573, 610	6.23	
(**10**)	263, 275, 305, 360, 440, 560, 610	1.69	
(**11**)	265, 298, 323	Diamag.	

Electron spin resonance (ESR)

To obtain further information about the stereochemistry and the nature the metal ligand bonding [25], ESR spectra of solid Mn complexes (**2**) and (**9**) and copper(II) complexes (**4**), (**5**), (**7**) and

(Table 5) have been carried out. The spectra of copper(II) complexes (**4**), (**5**), (**7**) and (**10**) showed that, the complexes exhibited anisotropic signals with $g_{\|}$ = (2.3-2.28) range, $g_{\perp}$ = (2.0-2.09) range. These values were characteristic for a species d^9 configuration with an axial symmetry type of dx^2-y^2 ground state with covalent bond character [26]. The g_{II}/A_{II} values (Table 5), indicating distorted octahedral geometry, however K and a value (Table 5) confirmed considerable covalent bond character. The in plane and out of-plane π bonding coefficient β^2 and β_1^2 bond character [27]. Also, the calculated orbital population a_d^2 for the cooper(II) complexes indicated ground state [3]. For the copper complex (**10**), the values of $g_{\|}$ and $g_{\perp}$ are closer to 2.00 and $g_{\perp} > g_{\|} > g_e$ (2.0023) indicating that, the complex possessed a compressed tetragonal distortion copper(II) geometry corresponding to an elongation along the four fold symmetry z-axis [28]. However, the spectra showed that, the complex (**2**) and (**9**) exhibited isotropic signals with g_{iso} values = 2.05 and 2.09, indicating distorted octahedral structure around Mn(II)ions with covalent bond character. The ESR data are shown in Table 5.

Table 5. ESR data for some metal(II) complexes.

No.	$g_{\|}$	$g_{\perp}$	g_{iso}[a]	$A_{\|}$ (G)	$A_{\perp}$ (G)	A_{iso}[b] (G)	G [c]	ΔE_{xy}	ΔE_{xz}	$K_{\perp}^2$	$K_{\|}^2$	K	K^2	$g_{\|}/A_{\|}$	α^2	β^2	β_1^2	-2 ß	a_d^2 (%)
(**4**)	2.3	2.09	2.16	1.25	5	45	3.3	17699	20920	1.11	0.79	1.0		177	0.73	1.52	1.08	167.6	52%
(**5**)	2.28	2.06	2.13	100	10	40	4.6	18691	21978	0.76	0.78	0.74	0.77	2.28	0.62	1.22	1.25	175.7	84.5%
(**7**)	2.25	2.08	2.13	120	75	45	3.13	17699	21505	1.01	0.66	0.51	0.89	187.5	0.65	1.55	1.01	289	89.1%
(**9**)	-	-	2.09	-	-	15	-	-	-	-	-	-	-	-	-	-	-	-	
(**10**)	2.15	2.33	2.27	130	10	50	-	-	-	-	-	-	-	-	-	-	-	-	-

Thermal analyses (DTA and TGA)

The thermal data of the complexes are given in Table 6. Such data corroborate the stoichiometric formula, number of water molecules, and end products [29]. Thermogravic curves of complexes (**2-6**), (**8**) and (**10-11**) were introduced as representative examples. Thermogram of complex (**2**): $[(HL)(Mn)(OAc)_2(H_2O)_2].H_2O$ exhibited five-steps decomposition, the first step involving breaking of H-bonding accompanied with endothermic peak appeared at 45 ºC. In the second step, one hydrated water molecule was lost endothermically with appearance of a peak at 80 ºC accompanied by 3.2% (calc 3.4%) weight loss. In the next step, two coordinated water molecules were lost endothermically with appearance of a peak at 120 ºC accompanied by 7.00% (calc 7.1%) weight loss. In the next step, two molecule of coordinated acetate (OAc) molecules were lost endothermically with appearance of a peak at 260 ºC accompanied by 25.00% (calc 25.05%) weight loss. The endothermic peak observed at 385 ºC refers to the melting point of the complex. The final step was observed as exothermic peaks at 440, 520, 620, 630, 650 ºC with 19.6% weight loss (calc 19.8%), referred to complete oxidative decomposition of the complex which ended up with the formation of (MnO).

Complex (3). $[(HL)(Ni)(OAc)_2(H_2O)_2].2H_2O$ exhibited multiple decomposition steps, the first step involving breaking of H-bonding accompanied with endothermic peak at 50 ºC. In the second step two molecules of hydrated water were lost endothermically with a peak at 85 ºC accompanied by 6.55% (calc 6.58%) weight loss, then two molecules of coordinated water were lost endothermically with a peak at 130 ºC accompanied by 7.2% (calc 7.04%) weight loss. 24.6% (calc 24.8%) weight loss accompanied by an endothermic peak appeared at 250 ºC was assigned to loss of two acetate (OAc) molecules. The endothermic peak appeared at 490 ºC referred to the melting point of the complex. The final step was observed as exothermic peaks at 450, 550, 600, 620, 620 ºC with 20.7% weight loss (calc 20.6%), refers to complete oxidative decomposition of the complex which ended up with the formation of (NiO).

*Complex (**4**)*. [(HL)(Cu)$(OAc)_2(H_2O)_2$].$2H_2O$ exhibited multiple decomposition steps, the first step involving breaking of H-bonding accompanied with endothermic peak at 45 ºC. In the second step 6.51% (calc 6.52%) weight loss accompanied by endothermic peaks appeared at 70 ºC of two molecules of hydrated water, then two molecules of coordinated water were lost endothermically with a peak at 145 ºC accompanied by 6.82% (calc.6.97%) weight loss and 210 ºC were assigned accompanied by 25.43% (calc %24.58) weight loss of two coordinated acetate (OAc). The endothermic peak observed at 390 ºC refers to the melting point of the complex. The final step observed as exothermic peaks at 430, 480, 500, 550, 660 ºC with 20.1% (calc 21.8%), refers to complete oxidative decomposition of the complex which ended up with the formation of (CuO).

*Complex (**5**)*. [(HL)$Br_2(H_2O)_2$].$2H_2O$ exhibited multiple decomposition steps, the first step involving breaking of H-bonding accompanied with endothermic peak at 40 ºC. In the second step, two molecules of hydrated water were lost endothermically with a peak at 65 ºC accompanied by 6.1% (calc 6.07%) weight loss. then two molecules of coordinated water were lost endothermically with a peak at 110 ºC accompanied by 6.39% (calc 6.46%) weight loss 30.51% (calc 30.71%) weight loss accompanied by an endothermic peak observed at 280 ºC was assigned to loss of two coordinated bromide group (Br) [30]. The endothermic peak observed at 360 ºC refers to the melting point of the complex. The final step observed a exothermic peaks at 420, 480, 560, 610, 640 ºC range with 21.65% weight loss (calc 21.88%), refers to complete oxidative decomposition of the complex which ended up with the formation of (CuO).

*Complex (**6**)*. [(HL)(Cd)$(Cl)_2$ $(H_2O)_2$].$2H_2O$ multiple decomposition steps, the first step involving breaking of H-bonding accompanied with endothermic peak at 30 ºC. In the second step, two molecule of hydrated water was lost endothermically with a peak at 75 ºC accompanied by 6.54% (calc 6.50%). then two molecules of coordinated water were lost endothermically with a peak at 135 ºC accompanied by 6.85% (calc. 6.96%) weight loss weight loss. 14.49% (calc 14.55%) weight loss accompanied by an endothermic peak at 295 ºC was assigned to loss of two coordinated chloride groups (Cl). The endothermic peak observed at 460 ºC refers to the melting point of the complex. The final step observed as exothermic peaks at 490, 520, 560, 600, 670 ºC with 30.9% weight loss (calc 31.1%), refers to complete oxidative decomposition of the chelate which ended up with the formation of (CdO).

*Complex (**8**)*. [(HL)(Ni)$(Cl)_2(H_2O)_2$].H_2O exhibited multiple decomposition steps, the first step involving breaking of H-bonding accompanied with endothermic peak at 45 ºC. In the second step one molecule of hydrated water was lost endothermically with a peak at 80 ºC accompanied by 3.6% (calc 3.73%) weight loss, then two molecules of coordinated water were lost endothermically with a peak at 120 ºC accompanied by 7.70% (calc 7.75%) weight loss 16.36% (calc 16.35%) weight loss accompanied by an endothermic peak at 260 ºC was assigned to loss of two chloride (Cl) molecules. The endothermic peak appeared at 410 ºC refers to the melting point of the complex. The final step was observed as exothermic peaks at 440, 520,620,630,650 ºC with 29.67% weight loss (calc 20.56%), refers to complete oxidative decomposition of the complex which ended up with the formation of (NiO).

*Complex (**10**)*. [(HL)(Cu)$(SO_4)(H_2O)_3$].$3H_2O$ exhibited multiple decomposition steps, the first step involving breaking of H-bonding accompanied with endothermic peak at 50 ºC. In the second step 9.52% (calc 9.54%) weight loss accompanied by endothermic peaks appeared at 85 ºC of two molecules of hydrated water, then three molecules of coordinated water were lost endothermically with a peak at 130 ºC accompanied by 10.50% (calc 10.54%) weight loss and 250 ºC were assigned accompanied by 21.1% (calc %20.9) weight loss of one coordinated sulfate (SO_4). The endothermic peak observed at 490 ºC refers to the melting point of the complex. The final step

observed as exothermic peaks at 450, 550, 600, 620, 620 ºC with 20.9% (calc 21.8%), refers to complete oxidative decomposition of the complex which ended up with the formation of (CuO).

*Complex (**11**)*. [(HL)(Zn)(SO_4)(H_2O)$_3$].3H_2O exhibited multiple decomposition steps, the first step involving breaking of H-bonding accompanied with endothermic peak at 45 ºC. In the second step, three molecules of hydrated water were lost endothermically with a peak at 70 ºC accompanied by 9.50% (calc 9.52%) weight loss. then three molecules of coordinated water were lost endothermically with a peak at 145 ºC accompanied by 10.63% (calc 10.52%) weight loss 21.4% (calc 20.9%) weight loss accompanied by an endothermic peak observed at 260 ºC was assigned to loss of one coordinated sulfate (SO_4) group [31]. The endothermic peak observed at 390 ºC refers to the melting point of the complex. The final step observed a exothermic peaks at 430, 480, 500, 550, 660 ºC with 22.3% weight loss (calc 21.9%), refers to complete oxidative decomposition of the complex which ended up with the formation of (ZnO).

Table 6. Thermal analysis of some complexes.

Compound No. molecular formula	Temperature (ºC) ºC	DTA (peak)		TGA (Wt. loss %)		Assignments
		Endo	Exo	Calc.	Found	
Complex (**2**)	45	Endo	-	-	-	Broken of H-bonding
	80	Endo		3.4	3.2	Loss of (H_2O) hydrated water molecules
	120	Endo	-	7.1	7.00	Loss of (2H_2O) coordinated water molecules
	260	Endo	-	25.05	25.00	Loss of coordinated (2OAc) group
	410	Endo		-	-	Melting point
	440, 520, 620, 630, 650	-	Exo	19.8	19.6	Decomposition process with the formation of (MnO)
Complex (**3**)	50	Endo	-	-	-	Broken of H-bonding
	85	Endo		6.58	6.55	Loss of (2H_2O) hydrated water molecules
	130	Endo	-	7.04	7.2	Loss of (2H_2O) coordinated water molecules
	250	Endo		24.8	24.6	Loss of coordinated (2OAc) group
	490	Endo	-	-	-	Melting point
	450,550,600, 620,620	-	Exo	20.7	20.6	Decomposition process with the formation of (NiO)
Complex (**4**)	45	Endo	-	-	-	Broken of H-bonding
	70	Endo		6.52	6.51	Loss of (2H_2O) hydrated water molecules
	145	Endo	-	6.97	6.82	Loss of (2H_2O) coordinated molecules
	260	Endo	-	24.58	25.43	Loss of coordinated (2OAc) group
	390	Endo	-	-	-	Melting point
	430,480,500, 550,660	-	Exo	21.8	20.1	Decomposition process with the formation of (CuO)
	40	Endo	-	-	-	Broken of H-bonding
	65	Endo		6.07	6.1	Loss of (2H_2O) hydrated water molecules

Complex (**5**)	110	Endo	-	6.46	6.39	Loss of ($2H_2O$) coordinated water molecules
	280	Endo	-	30.71	30.51	Loss of coordinated (2Br) group
	360	Endo	-	-	-	Melting point
	420,480,560, 610,640	-	Exo	21.88	21.65	Decomposition process with the formation of (CuO)
Complex (**6**)	30	Endo	-	-	-	Broken of H-bonding
	75	Endo		6.50	6.54	Loss of ($2H_2O$) hydrated water molecules
	135	Endo	-	6.96	6.85	Loss of ($2H_2O$) coordinated water molecules
	295	Endo	-	14.55	14.49	Loss of coordinated (2Cl) group
	460	Endo	-	-	-	Melting point
	490,520,560, 600,670	-	Exo	31.1	30.9	Decomposition process with the formation of (CdO)
Complex (**8**)	45	Endo	-	-	-	Broken of H-bonding
	80	Endo		3.73	3.6	Loss of (H_2O) hydrated water molecules
	120	Endo	-	7.75	7.70	Loss of ($2H_2O$) coordinated water molecules
	260	Endo	-	16.35	16.36	Loss of coordinated (2 Cl) group
	410	Endo		-	-	Melting point
	440,520,620, 630,650	-	Exo	29.67	20.56	Decomposition process with the formation of (NiO)
Complex (**10**)	50	Endo	-	-	-	Broken of H-bonding
	85	Endo		9.54	9.52	Loss of ($3H_2O$) hydrated water molecules
	130	Endo	-	10.54	10.50	Loss of ($3H_2O$) coordinated water molecules
	250	Endo		20.9	21.1	Loss of coordinated (SO_4) group
	490	Endo	-	-	-	Melting point
	450,550,600, 620,620	-	Exo	21.8	20.9	Decomposition process with the formation of (CuO)
Complex (**11**)	45	Endo	-	-	-	Broken of H-bonding
	70	Endo		9.52	9.50	Loss of ($3H_2O$) hydrated water molecules
	145	Endo	-	10.52	10.63	Loss of ($3H_2O$) coordinated molecules
	260	Endo	-	20.9	21.4	Loss of coordinated (SO_4) group
	390	Endo	-	-	-	Melting point
	430,480,500, 550,660	-	Exo	22.3	21.9	Decomposition process with the formation of (ZnO)

Antimicrobial activity

The antimicrobial activity of the ligand (**1**) and some of its complexes were examined against *Bacillus subtilis*, *Staphylococcus aureus*, *Escherichia coli* and *Pseudomonas aeruginosa;* the results were listed in Table 7. All the tests were performed in triplicate and the diameters of the inhibition zones were measured in millimeters. The drugs ampicillin and kanamycin were taken as standard to compare the effectiveness of the test compounds. The effectiveness of the compound can be predicated by knowing the zone of inhibition value in mm. The antibacterial activity was then interpreted as followed: The diameter of inhibition zone > 15.0 mm was considered as strong; 10.0 to 14.5 mm as moderate and <10.0 as weak. It was found that most

compounds exhibit strong biocide activity against the other tested types of microbes (Figures 3 and 4). The ligand showed the least antimicrobial activity against the four types microbes: *Bacillus subtilis*, *Staphylococcus aureus*, *Escherichia coli* and *Pseudomonas aeruginosa* with an inhibition zone ranging from (11-13) mm. For metal complexes, Mn(II) complex (**2**) represented the most sensitive complex against *Bacillus subtilis*, *Staphylococcus aureus*, *Escherichia coli* and *Pseudomonas aeruginosa* with 21, 25, 21, 22, mm, respectively, inhibition zone whereas, Zn(II) complex (**10**) recorded the highest antimicrobial activity against *Streptococcus aureus*. The orders of the antimicrobial activity were as follow: *Bacillus subtilis*: standard drug > Mn(II) complex **(2)** > Zn(II) complex **(11)** > Cd(II) complex (**6**) > Cu(II) complex (**5,7**) > Cu(II) complex (**4**) > Cu(II) complex **(10)** > The ligand [L] (**1**).

Staphylococcus aureus. Standard drug > Zn(II) complex (**11**) > Mn(II) complex **(2)** > Cd(II) complex (**6**) > Cu(II) complex (**5,7**) > Cu(II) complex **(10)** > The ligand [L] (**1**).

Escherichia coli. Standard drug > Zn(II) > Mn(II) > complex (**2,11**) > Cu(II) complex (**7**) > Cd(II) complex **(6)** > Cu(II) complex (**5**) > Cu(II) complex (**10**) > Cu(II) complex **(4)** > The ligand [L] (**1**).

Pseudomonas aeruginosa. Standard drug > Zn(II) complex (**11**) > Mn(II) complex (**2**) > Cu(II) complex (**7**) > Cu(II) > Cd(II) complex **(5,6)** > Cu(II) complex(**10**) > Cu(II) complex **(4)** > The ligand [L] (**1**).

Metal complexes have specific steric and electronic effects that lead to different mechanisms of action (e.g. electron transferee and redox process [32]. Metal, because of being less electronegativity tends to promptly form positively charged ions and this properly lends them greater solubility in the biological fluids [33]. The positively charged ions thus formed have affinity for electron-rich biomolecules such as DNA and proteins and play role in stabilizing and influencing in structure [34]. The metal complexes showed antibacterial activity against different bacteria probably by intercalating with DNA or by disrupting the cell membrane [35]. For copper(II) complexes, the exact mechanism of antimicrobial, many investigations have shown that reactive oxygen species (ROS) produced through Fenton-Type [36].

Reactions damage DNA

The release of copper ions causes inactivation of enzymes that leads to its toxicity for Zn(II) and Cd(II) complexes, it was inhibited the growth of bacteria through two modes of its action. Direct action where by microbial membrane is destabilized and its permeability is increased [37] and indirect action, whereby interaction with nucleic acids leads to deactivation of respiratory enzymes [38].

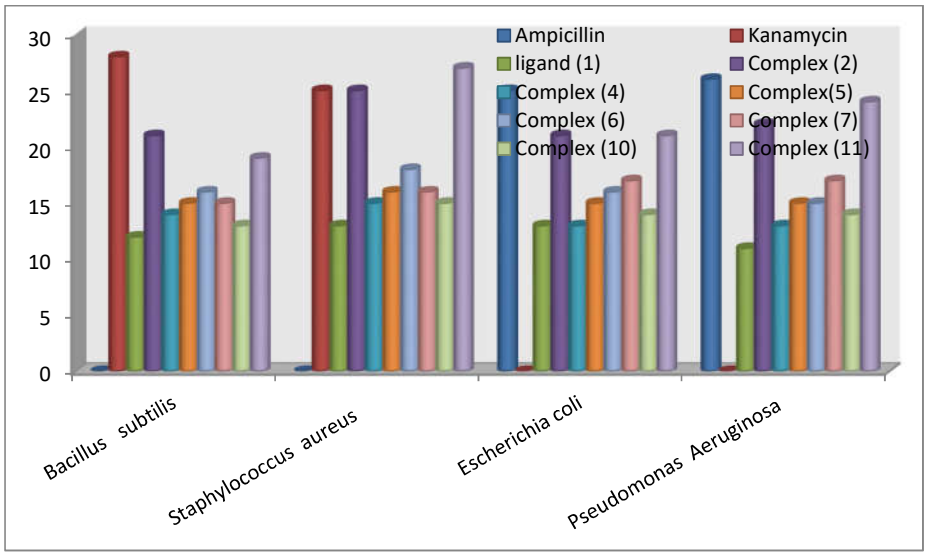

Figure 2. Antimicrobial activity of ligand and some of its metal complex.

Table 7. Evaluation of *in vitro* antibacterial activity of compounds ligand and complexes (**2**, **4**, **5**, **6**, **7**, **10** and **11**) against gram-positive and gram-negative bacterial strains of clinical importance using disc diffusion test.

Compounds	Zone of inhibition in mm			
	Gram positive bacteria[a]		Gram negative bacteria[b]	
Empty cell	*B. S.*	*S. A.* (MRSA)	*E. C.*	*P. A.*
Ligand	11 ± 1	14 ± 1	12 ± 2	10 ± 1
Complex (**2**)	22± 1	25	21 ± 1	23 ± 3
Complex (**4**)	14 ± 1	15± 2	13 ± 1	12 ± 2
Complex (**5**)	15 ± 1	15 ± 1	15 ± 1	14 ± 2
Complex (**6**)	16 ± 1	17 ± 1	15 ± 1	14 ± 1
Complex (**7**)	15± 1	16±2	18±2	17±2
Complex (**10**)	13±2	12±1	14±1	13±1
Complex (**11**)	19±1	27±1	21±1	25
Ampicillin	–	–	25 ± 2	28 ± 1
Kanamycin	29 ± 1	28 ± 1	–	–

Kanamycin (positive controls) and Ampicillin (negative control). [a]Gram-positive bacterium: *S. A.* (MRSA) - *Staphylococcus aureus* (*Methicillin-resistant)*, *B. S.* – *Bacillus subtilis*, - [b]Gram negative bacteria: *E. C.* - *Escherichia coli*, *P. A.* – *Pseudomonas aeruginosa*.

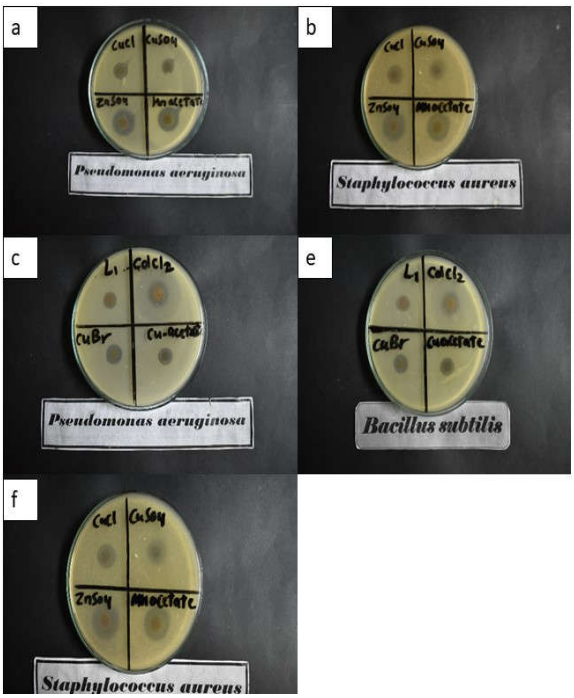

Figure 3. (a, b, c, e and f) Inhibition zones for ligand and some metal complexes against *Staphylococcus aureus*, *Bacillus subtilis*, *Escherichia coli* and *Pseudomonas aeruginos*.

CONCLUSION

In the present study, new metal(II) complexes derived N-(2-aminophenyl)-4-(pentyloxy)benzamide ligand were prepared. Structural and spectroscopic properties revealed that the ligand adopted a tridentate fashion; on the other hand the metal complexes adopted a tetragonal distorted octahedral geometry around metal ions. All the complexes are non-electrolytic in nature as suggested by molar conductance measurements. The ligand coordinated to the central metal ion through a carbonyl group, one-amine nitrogen, forming ring including the metal ions. The antimicrobial activities of the ligand as and its metal complex were assessed against: *Staphylococcus aureus*, *Bacillus subtilis*, *Escherichia coli*, and *Pseudomonas aeruginosa*. Results showed that metal complexes are moderate active against both *Bacillus subtilis* and *Escherichia coli.* On the other hand, they demonstrated more potent antimicrobial activity against *Staphylococcus aureus* and *Pseudomonas Aeruginosa.*

REFERENCES

1. Awasthi, D.K.; Gupta, S.; Awasthi, G. Application of transition metal complex in medicine. *World J. Pharm. Med. Res.* **2019**, 5, 54-84.
2. Liang, X.; Luan, S.; Yin, Z.; He, M.; He, C.; Yin, L.; Zou, Y.; Yuan, Z.; Li, L.; Song, X.; Lv, C.; Zhang, W. Recent advances in the medical use of silver complex. *Eur. J. Med. Chem.* **2018**, 157, 62-80.
3. Jabarah, Z.A.; Fayad, A.A.; Al-Kadi, I.S.A. Design, synthesis, spectral characterization, and study of biological effect of novel azobenzen-p,p'-di(2-amine-1,3,4-thiadiazol-5-yl) derivatives. *Synthesis* **2017**, 17, 18.
4. Dalle, K.E.; Meyer, F. Modelling binuclear metallobiosites: insights from pyrazole-supported biomimetic and bioinspired complexes. *Eur. J. Inorg. Chem.* **2015**, 2015, 3391-3405.
5. Hazra, M.; Dolai, T.; Giri, S.; Patra, A.; Dey, S.K. Synthesis of biologically active cadmium(II) complex with tridentate N2O donor Schiff base: DFT study, binding mechanism of serum albumins (bovine, human) and fluorescent nanowires. *J. Saudi Chem. Soc.* **2017**, 21, S445-S456.
6. Liang, J.W.; Wang, Y.; Du, K.J.; Li, G.Y.; Guan, R.L.; Ji, L.N.; Chao, H. Synthesis, DNA interaction and anticancer activity of copper(II) complexes with 4′-phenyl-2,2′:6′,2″-terpyridine derivatives. *J. Inorg. Biochem.* **2014**, 141, 17-27.
7. Bhagwatrao Biradar, S.; Vithal Narte, D.; Pradip Kale, R.; Momin, K.I.; Sudewad, M.S.; Tayade, K.C.; Palke, D.G. Synthesis, spectral and biological studies of DHA Schiff bases. *J. Appl. Organometal. Chem.* **2021**, 1, 41-47.
8. Meena, K.; Kumar Baroliya, P. Synthesis, characterization, antimicrobial and antimalarial activities of azines based Schiff bases and their Pd(II) complexes. *Chem. Biodiver.* **2023**, 20, e202300158.
9. Baddar, F.G.; Hilal, O.M.M.; Sugden, S. The determination of magnetic susceptibility by the Gouy method. *J. Chem. Soc. (Resumed)* **1949**, 2, 132-135.
10. Vogel, A.I. *Macro and Semimicro Qualitative Inorganic Analyses*, Longmans: London; **1954**; p. 663.
11. EL-Table, A.S.; Wassel, M.A.; Arafa, M.M.; Alhalib, A.A.; Wassel, A.A. Thermal analyses (DTA and TGA) of ligand (H_6L) and its metal complexes Co(II), Fe(II), Cu(II) and Ni(II*). Int J. Sci. Eng. Res.* **2017**, 8, 2044-2052.,
12. Dalle, K.E.; Meyer, F. Modelling binuclear metallobiosites: insights from pyrazole-supported biomimetic and bioinspired complexes. *Eur. J. Inorg. Chem.* **2015**, 2015, 3391-3405.
13. Rouzer, C.A. Metals and DNA repair. *Chem. Res. Toxicol.* **2010**, 23, 1517-1518.
14. Bauer, A.W. Antibiotic susceptibility testing by a standardized single disk method. *Am. J. Clin. Path.* **1966**, 45, 493-496.
15. Veeravel, C.; Selvarani, R. Ex-vivo antimalarial and in-vitro biological activities of newly synthesized Co(II) complex with Schiff base. *Egypt. J. Chem*. **2021**, 64, 4191-4195.
16. Ghoneim, M.M.; El-Sonbati, A.Z.; El-Bindary, A.A.; Diab, M.A.; Serag, L.S. Polymer complexes. LX. Supramolecular coordination and structures of N(4-(acrylamido)-2-hydroxybenzoic acid) polymer complexes. *Spectrochim. Acta A: Mol. Biomol. Spectrosc.* **2015**, 140, 111-131.
17. Ghoneim, M.M.; El-Sonbati, A.Z.; El-Bindary, A.A.; Diab, M.A.; Serag, L.S. Polymer complexes. LX. Supramolecular coordination and structures of N(4-(acrylamido)-2-hydroxybenzoic acid) polymer complexes. *Spectrochim. Acta - A: Mol. Biomol. Spectrosc.* **2015**, 140, 111-131.
18. Rosu, T.; Pahontu, E.; Pasculescu, S.; Georgescu, R.; Stanica, N.; Curaj, A.; Popescu, A.; Leabu, M. Synthesis, characterization antibacterial and antiproliferative activity of novel Cu(II) and Pd(II) complexes with 2-hydroxy-8-R-tricyclo [7.3.1.0.2,7] tridecane-13-one thiosemicarbazone. *Eur. J. Med. Chem*. **2010**, 45, 1627-1634.

19. El-Tabl, A.S.; El-Saied, F.A.; Al-Hakimi, A.N. Spectroscopic characterization and biological activity of metal complexes with an ONO trifunctionalized hydrazone ligand. *J. Coord. Chem.* **2008**, 61, 2380-2401.
20. Kouser, R.; Zehra, S.; Khan, R.A.; Alsalme, A.; Arjmand, F.; Tabassum, S. "Turn–on" benzophenone based fluorescence and colorimetric sensor for the selective detection of Fe^{2+} in aqueous media: Validation of sensing mechanism by spectroscopic and computational studies. *Spectrochim. Acta - A: Mol. Biomol. Spectrosc.* **2021**, 247, 119156.
21. Sail, B.S.; Naik, V.H.; Prasanna, B.M., Ahmad, N.; Khan, M.R.; Jagadeesh, M.R.; Cheedarala, R. Synthesis, characterization and pharmacological studies of cobalt(II), nickel(II) and copper(II) complexes of thiazole Schiff bases. *J. Mol. Struct*. **2023**, 1288, 135748.
22. Kouser, R.; Zehra, S.; Khan, R.A.; Alsalme, A.; Arjmand, F.; Tabassum, S. "Turn–on" benzophenone based fluorescence and colorimetric sensor for the selective detection of Fe^{2+} in aqueous media: Validation of sensing mechanism by spectroscopic and computational studies. *Spectrochim. Acta - A: Mol. Biomol. Spectrosc.* **2021**, 247, 119156.
23. El Tabl, A.; Abd Wlwahed, M.; Abd-Elwareth, M.; Faheem, S. Nano metal complexes in cancer therapy, preparation, spectroscopic, characterization and anti-breast cancer activity of new metal complexes of alanine Schiff-base. *Egypt. J. Chem*. **2021**, 64, 3131-3152.
24. El-Tabl, A.S.; Shakdofa, M.M.; Shakdofa, A.M. Metal complexes of N'-(2-hydroxy-5-phenyldiazenyl) benzylideneisonicotinohydrazide: Synthesis, spectroscopic characterization and antimicrobial activity. *J. Serb. Chem. Soc*. **2013**, 78, 39-55.
25. Shohayeb, S.M.; Mohamed, R.G.; Moustafa, H.; El-Medani, S.M. Synthesis, spectroscopic, DFT calculations and biological activity studies of ruthenium carbonyl complexes with 2-picolinic acid and a secondary ligand. *J. Mol. Struct*. **2016**, 1119, 442-450.
26. Muniyandi, V.; Pravin, N.; Subbaraj, P.; Raman, N. Persistent DNA binding, cleavage performance and eco-friendly catalytic nature of novel complexes having 2-aminobenzophenone precursor. *J. Photochem. Photobiol. B.* **2016**, 156, 11-21.
27. Nnabuike, G.G.; Salunke-Gawali, S.; Patil, A.S.; Butcher, R.J.; Obaleye, J.A.; Ashtekar, H.; Prakash, B. Copper(II) complexes containing derivative of aminobenzoic acid and nitrogen-rich ligands: Synthesis, characterization and cytotoxic potential. *J. Mol. Struct.* **2023**, 1279, 135002.
28. Illán-Cabeza, N.A.; García-García, A.R.; Moreno-Carretero, M.N.; Martínez-Martos, J.M.; Ramírez-Expósito, M.J. Synthesis, characterization and antiproliferative behavior of tricarbonyl complexes of rhenium(I) with some 6-amino-5-nitrosouracil derivatives: Crystal structure of fac-[$ReCl(CO)_3$(DANU-N5,O4)] (DANU = 6-amino-1,3-dimethyl-5-nitrosouracil). *J. Inorg. Biochem.* **2005**, 99, 1637-1645.
29. EL-Table, A.S.; Wassel, M.A.; Arafa, M.M.; Alhalib, A.A.; Wassel, A.A. Thermal analyses (DTA and TGA) of ligand (H_6L) and its metal complexes Co(II), Fe(II), Cu(II) and Ni(II). *Int. J. Sci. Eng. Res.* **2017**, 11, 2044-2052.
30. Zhao, Y.L.; Yang, T.; Tong, Y.; Wang, J.; Luan, J.H.; Jiao, Z.B.; Chen, D.; Yang, Y.; Hu, A.; Liu, C.T.; Kai, J.-J. Recent advances in the medical use of silver complex. *Eur. J. Med. Chem.* **2018**, 157, 62-80.
31. Youngs, W.J.; Knapp, A.R.; Wagers, P.O.; Tessier, C.A. Nanoparticle encapsulated silver carbene complexes and their antimicrobial and anticancer properties: a perspective. *Dalton Trans.* **2012**, 41, 327-336.
32. Macomber, L.; Imlay, J.A. The iron-sulfur clusters of dehydratases are primary intracellular targets of copper toxicity. *Proc. Natl. Acad. Sci.* **2009**, 106, 8344-8349.
33. Fang, M.; Chen, J.H.; Xu, X.L.; Yang, P.H.; Hildebrand, H.F. Antibacterial activities of inorganic agents on six bacteria associated with oral infections by two susceptibility tests. *Int. J. Antimicrob. Agents* **2006**, 27, 513-517.

34. Singh, A.; Prasad, L.B.; Shiv, K.; Kumar, R.; Garai, S. Synthesis, characterization, and in vitro antibacterial and cytotoxic study of Co(II), Ni(II), Cu(II), and Zn(II) complexes of N-(4-methoxybenzyl) N-(phenylethyl) dithiocarbamate ligand. *J. Mol. Struct*. **2023**, 1288, 135835.
35. Chaudhary, A. Synthesis, spectroscopic elucidation, in vitro antimicrobial, cytotoxic and CT-DNA binding evaluation of heterobimetallic complexes of Ni(II) with main group/transition metal dichlorides. *J. Mol. Struct*. **2023**, 1279, 134936.
36. Husain, A.Z.; Al-Jawaheri, Y.S.; Al-Assafe, A.Y. Synthesis of substituted heterocyclic with their cobalt(II) complexes from 2-amino-thiazoles and evaluation of their biological activity. *Bull. Chem. Soc. Ethiop*. **2024**, 38, 909-922.
37. Al-Assafe, A.Y.; Al-Quaba, R.A. Synthesis, characterization and antibacterial studies of ciprofloxaci-imines and their complexes with oxozirconium(IV), dioxomolybdenum(VI), and dioxotungsten(VI). *Bull. Chem. Soc. Ethiop.* **2024**, 38, 949-962.
38. Al-Assafe, A.Y.; Al-Quaba, R.A. Synthesis, characterization, and antibacterial studies of some of first transition series metals and zinc complexes with mixed ligands of trimethoprim-isatin and nitrogen base. *Bull. Chem. Soc. Ethiop.* **2024**, 38, 1013-1025.